Inhibition of Soluble Guanylate Cyclase by ODQ†

Yunde Zhao,‡ Philip E. Brandish,‡ Marilena DiValentin,§ Johannes P. M. Schelvis,§ Gerald T. Babcock,*,§ and Michael A. Marletta*,‡,||,⊥

Department of Biological Chemistry, School of Medicine, Howard Hughes Medical Institute, and Department of Medicinal Chemistry, College of Pharmacy, The University of Michigan, Ann Arbor, Michigan 48109-0606, Department of Chemistry, Michigan State University, East Lansing, Michigan 48824-1322

Received December 22, 1999; Revised Manuscript Received June 26, 2000

ABSTRACT: The heme in soluble guanylate cyclases (sGC) as isolated is ferrous, high-spin, and 5-coordinate. [1*H*-[1,2,4]oxadiazolo-[4,3-*a*]quinoxalin-1-one] (ODQ) has been used extensively as a specific inhibitor for sGC and as a diagnostic tool for identifying a role for sGC in signal transduction events. Addition of ODQ to ferrous sGC leads to a Soret shift from 431 to 392 nm and a decrease in nitric oxide (NO)-stimulated sGC activity. This Soret shift is consistent with oxidation of the ferrous heme to ferric heme. The results reported here further define the molecular mechanism of inhibition of sGC by ODQ. Addition of ODQ to the isolated sGC heme domain [β1(1−385)] gave the same spectral changes as when sGC was treated with ODQ. EPR and resonance Raman spectroscopy was used to show that the heme in ODQ-treated β1(1−385) is indeed ferric. Inhibition of the NO-stimulated sGC activity by ODQ is due to oxidation of the sGC heme and not to perturbation of the catalytic site, since the ODQ-treated sGC has the same basal activity as untreated sGC (68 ± 12 nmol min^{-1} mg^{-1}). In addition, ODQ-oxidized sGC can be re-reduced by dithionite, and this re-reduced sGC has identical NO-stimulated activity as the original ferrous sGC. Oxidation of the sGC heme by ODQ is fast with a second-order rate constant of 8.5×10^3 M^{-1} s^{-1}. ODQ can also oxidize hemoglobin, indicating that the reaction is not specific for the heme in sGC versus that in other hemoproteins.

cGMP[1] is a key component in the regulation of vasodilation, platelet aggregation, neuronal signaling, and retinal phototransduction and is produced by guanylate cyclase [GTP pyrophosphate-lyase (cyclizing), EC 4.6.1.2] (*1*, *2*). There are two types of guanylate cyclases: membrane-bound particulate guanylate cyclase (pGC) and soluble guanylate cyclase (sGC). Both pGC and sGC catalyze the same reaction involving the conversion of guanosine 5′-triphosphate (GTP) to guanosine 3′,5′-monophosphate (cGMP) and pyrophosphate; however, they are regulated quite differently. The activity of pGC is stimulated by small peptide hormones such as atrial natriuretic factor, while sGC is activated by nitric oxide (NO). pGC and sGC share a homologous catalytic domain that also shows some homology to the catalytic domains of adenylate cyclase (AC). It is believed that all nucleotide cyclases evolved from the same ancestral gene and use similar catalytic mechanisms. sGC is a heterodimeric hemoprotein consisting of the α1- and β1-subunits when isolated from lung tissue (*3*, *4*). The heme-binding region is at the N-terminal region of the β1-subunit (*5*−*7*), while the catalytic site is at the C-terminal region. The catalytic site is composed of residues from both subunits (*8*). Activation of sGC by NO is mediated by NO binding to the heme moiety in sGC (*9*, *10*).

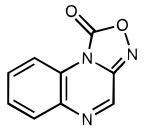

FIGURE 1: Structure of ODQ (1*H*-[1,2,4]oxadiazolo-[4,3-*a*]quinoxalin-1-one).

Compounds that selectively modulate the activity of specific isoforms of guanylate cyclases would be useful in the study of the physiological functions of these enzymes. Recently, ODQ (1*H*-[1,2,4]oxadiazolo-[4,3-*a*]quinoxalin-1-one, Figure 1) and its 8-bromo analogue NS-2028 were shown to inhibit NO-stimulated sGC activity (*11*−*13*). This compound does not affect the activity of either pGC or AC. Thus, ODQ seems to be a sGC-specific cyclase inhibitor and has been used extensively to study the function of the NO/cGMP signal transduction pathway. Although many studies involving ODQ have been published, the detailed inhibition mechanism of sGC inhibition by ODQ is not fully understood. Treatment of sGC with ODQ has been reported to shift the Soret peak from 431 to 392 nm, suggesting that the heme in sGC has been oxidized (*14*). The goal of this study is to further define the molecular mechanism of inhibition of sGC by ODQ. We find that ODQ reacts with the ferrous

† The studies were supported by Howard Hughes Medical Institute, Predoctoral Fellowship from the Graduate School of the University of Michigan and NIH Grant GM25480.

* To whom correspondence should be addressed.
‡ Department of Biological Chemistry.
|| Howard Hughes Medical Institute.
⊥ Division of Medicinal Chemistry.
§ Department of Chemistry, Michigan State University.

[1] Abbreviations: AC, adenylate cyclase; cGMP, cyclic guanosine 3′,5′-monophosphate; DTT, dithiothreitol; EPR, electron paramagnetic resonance; GTP, guanosine 5′-triphosphate; IBMX, isobutylmethylxanthine; NO, nitric oxide; ODQ, 1*H*-[1,2,4]oxadiazolo-[4,3-*a*]quinoxalin-1-one; PMSF, phenylmethanesulfonyl fluoride; sGC, soluble guanylate cyclase.

10.1021/bi9929296 CCC: $19.00
Published on Web 08/08/2000

heme of sGC to yield ferric heme. ODQ does not adversely affect the catalytic domain of sGC, and re-reduction of the heme completely restores NO sensitivity. We also find that ODQ is able to oxidize hemoglobin, showing that the reaction is not specific for sGC among hemoproteins.

MATERIALS AND METHODS

Materials. β1(*1*− 385) was expressed in *Escherichia coli* and purified as previously described (*6*). cGMP EIA kits were purchased from Biomol. ODQ and all other chemicals were from Sigma unless otherwise stated. Unless specified, all experiments were carried out aerobically.

Cell Culture. Fall army worm ovary cells (*Spodoptera frugiperda*, Sf9) were grown at 28 °C in monolayer and suspension cultures in Grace's modified insect medium (Gibco BRL #11605−094) supplemented with 10% fetal calf serum (Hyclone #A-1115-N), 0.1% Pluronic F-68, and 1× antibiotic (Gibco BRL # 15240−062). Monolayer cultures were grown in Costar or Corning tissue culture flasks and suspension cultures in 500-mL Erlenmeyer flasks (Bellco Glass, Inc.) with shaking at 110 rpm. In suspension culture, cells were subcultured between 1×10^6 and 4×10^6 cells/mL. Cell density and viability were determined by trypan blue exclusion using a hemocytometer.

Infection of Sf9 Cells with Baculoviruses. Recombinant baculoviruses containing the cDNAs for the α1- and β1-subunits of rat lung sGC have been described previously (*15*). High-titer viral stocks were prepared by standard methods. The optimal amount of virus used of each stock (virus containing the α1- or β1-subunit cDNA) was determined by infecting a series of monolayer cultures with a fixed amount of α1-virus and varying amounts of β1-virus. Guanylate cyclase activity in the cytosolic fraction was determined as described previously (*16*). The ratio of viruses that gave the most activity was used. In a second series of infections, the ratio of viruses was fixed and the total amount added was varied. The optimal amount was assessed by sGC activity. For production of proteins, Sf9 cells were grown to 4×10^6 cells/mL in suspension cultures. The cells were collected by centrifugation and resuspended to a density of 2×10^6 cells/mL in medium (typically 2 L) containing the recombinant viruses. Cells were harvested 3 days post-infection by centrifugation, and the pellet was stored at −80 °C.

Purification of sGC. The following method is a modification of a previously reported method (*16*). The final step in this purification is gel filtration, providing the opportunity to isolate the protein in a buffer of choice. Cells from 2 L of cultures were thawed and resuspended in buffer 1 (20 mM KPi, pH 7.4, 25 mM NaCl, 5 mM DTT, 0.5 mM PMSF, 1 mM benzamidine, 0.1% CLAP [0.5 mg/mL chymostatin, 1 mg/mL leupeptin, 1 mg/mL antipain, and 1 mg/mL pepstatin A dissolved in DMSO], 75 mL) and broken using a Bead Beater (BioSpec Products) using 0.1-mm diameter glass beads. The lysate was centrifuged at 100000*g* for 90 min, and the supernatant was applied to a 75-mL (15 × 2.5 cm) column of ceramic hydroxyapatite (type II, 40 μm, BioRad Laboratories) equilibrated with buffer 1 at 1 mL/min using a BioRad Econo-system. The column was washed with buffer 1 (225 mL) and developed with a 20−200 mM phosphate gradient (300 mL) in buffer 1, collecting 7-mL fractions. Fractions containing sGC (identified by the heme Soret at 431 nm) were pooled, concentrated to 1−2 mL in an Ultrafree-15 100K filter (Millipore), and exchanged into buffer 2 (25 mM TEA, pH 7.4, 50 mM NaCl, 5 mM DTT, 1 mM EDTA, 0.5 mM PMSF, 1 mM benzamidine, 0.1% CLAP) using a Pharmacia PD-10 column. The sample was diluted to 9 mL with buffer 2 and applied to a 12-mL (6.8 × 1.5 cm) column of Q-Sepharose (Pharmacia) at 0.4 mL/min. The column was washed with buffer 2 (24 mL) and developed with a 50−400 mM gradient of NaCl (48 mL) in buffer 2, collecting 1.2-mL fractions. Fractions with A_{280}/A_{431} ratio <3.5 were pooled and concentrated to 0.5 mL using an Ultrafree-15 50K filter. The sample was applied to a column of Superdex-200 (60 × 1.6 cm, prepacked, Pharmacia) equilibrated with buffer 3 (50 mM HEPES, pH 7.4, 100 mM NaCl, 5 mM DTT, 1 mM EDTA, 0.5 mM PMSF, 1 mM benzamidine, 0.1% CLAP) at 1 mL/min using a BioRad BioLogic system. The column was washed with buffer 3, collecting 1-mL fractions. Fractions containing purified sGC were pooled, concentrated in an Ultrafree-15 50K filter, frozen by dripping directly into liquid N_2, and then stored in liquid N_2.

Electronic Absorption Spectral Studies of ODQ-Oxidized sGC and β1(1−385). sGC (500 μL, 1.8 μM) and a solution containing ODQ (1 μL, 1 mM in DMSO) were thoroughly mixed in a cuvette at room temperature. The reaction of ODQ with sGC was monitored by electronic absorption spectroscopy using a Cary 3E spectrophotmeter at room temperature. β1(1−385) (400 μL, 13.2 μM) and ODQ (2 μL, 5 mM in DMSO) were mixed in a cuvette. This reaction was also monitored by electronic absorption spectroscopy at 10 °C. The anaerobic oxidation of β1(1−385) was followed as described above except that stock solutions of ODQ and β1-(1−385) were prepared by 10 cycles of alternate evacuation and purging with purified argon gas using an oxygen-scavenged manifold. The manifold contained two in-line oxygen scrubbers (Oxiclear, Anspec) and one indicating scrubber (Oxisorb-Glass, Anspec). Oxygen levels are reduced to about 50 nM.

Oxidation of Ferrous Oxyhemoglobin with ODQ. Ferrous oxyhemoglobin (Sigma H-0267, 400 μL, 8 μM) was mixed with ODQ (4 μL, 25 mM in DMSO) in a cuvette at room temperature. Oxidation of the heme was monitored by electronic absorption spectroscopy.

sGC Activity Measurements. sGC activity was determined essentially as described previously (*16*) except that the GTP-regenerating system (creatine phosphate and creatine phosphate kinase) and the phosphodiesterase inhibitor IBMX were omitted. DEA-NONOate (Cayman Chemical, Ann Arbor, MI), dissolved to 10 mM in 10 mM NaOH, was used as a source of NO (1 mM final concentration). The assay mixture contained 50 mM Hepes, pH 7.4, 5 mM $MgCl_2$, and 1.5 mM GTP plus other materials as described in a final volume of 0.1 mL. The assay mixture was incubated at 37 °C for 1 min. Assays were started by addition of enzyme and were stopped after 2 min by addition of 125 mM $Zn(OAc)_2$ (0.4 mL) followed by 125 mM Na_2CO_3 (0.5 mL). cGMP was quantified using a cGMP EIA kit (Biomol) following the supplier's instructions. To study the effects of ODQ or potassium ferricyanide on the activity of sGC, sGC was preincubated with 1.5 equiv of ODQ or potassium ferricyanide at 25 °C for 5 min. After preincubation, ODQ or ferricyanide was removed by desalting into 50 mM Hepes,

pH 7.4, 50 mM NaCl using a PD-10 disposable gel-filtration column. The ODQ- or ferricyanide-treated sGC was assayed as described above. To assess the effect of ODQ on basal sGC activity, ODQ dissolved in DMSO was added to assays as described above. The final concentration of DMSO was 2%.

Reversibility of ODQ Inhibition. sGC was oxidized by ODQ as described above. The mixture of sGC and ODQ was then desalted into 50 mM Hepes, pH 7.4, and 50 mM NaCl using a PD-10 column. The sGC sample was then divided into two aliquots, one was assayed in the presence and absence of NO, and the other was re-reduced by dithionite, desalted, and assayed in the presence and absence of NO. The re-reduced sGC was also monitored spectroscopically in a Cary 3E spectrophotometer.

To characterize the reaction of ferric sGC with NO at 10 °C, ferricyanide- or ODQ-treated sGC was desalted into 50 mM Hepes, pH 7.4, and 50 mM NaCl and made anaerobic in a cuvette using a conventional gas train. Increasing amounts of NO gas were added, and finally, the headspace was purged with NO gas directly. To monitor changes in the absorbance and EPR spectra of ODQ-treated sGC in the presence of 1 mM DEA-NONOate under turnover conditions, ODQ-treated sGC was desalted into 50 mM Hepes, pH 7.4, and 50 mM NaCl and brought to 37 °C. GTP, $MgCl_2$, and DEA-NONOate were added to the same final concentrations as in the assays described above. The sample was transferred to a cuvette at 37 °C, and the absorbance spectrum was recorded 2 min post-mixing. The sample was then chilled on ice, and glycerol was added to 10% (v/v) final concentration. The sample was transferred to an EPR tube and frozen in liquid N_2. The EPR conditions were as follows: temperature, 25 K; microwave frequency, 9.5 GHz; power, 2 mW; and modulation amplitude, 4 G.

EPR Characterization of ODQ-Oxidized β1(1−385). EPR spectra were recorded using a Bruker ESP300E X-band spectrometer equipped with a standard TE102 rectangular cavity and an Oxford Instruments ESR-9 helium flow cryostat. ODQ (2 μL, 64 mM in DMSO) was mixed with β1(1−385) (400 μL, 160 μM) in an EPR tube. The buffer composition was 50 mM Hepes, pH 7.4, 100 mM NaCl, and 10% glycerol. EPR experimental conditions were as follows: temperature, 10 K; microwave frequency, 9.477 GHz; microwave power, 20 mW; modulation amplitude, 32 G. EPR spectra were simulated using the program Simfonia (version 1.0) from Bruker. EPR spectra of the same EPR sample described above were collected at higher temperature (80 K). Other experimental parameters were as follows: microwave frequency, 9.5 GHz; microwave power, 20 mW; modulation amplitude, 2 G.

Resonance Raman Characterization of the ODQ-Oxidized β1(1−385). β1(1−385) (200 μL, 25 μM) and ODQ (2 μL, 3 mM in DMSO) were mixed in a spinning cell. The resonance Raman spectra were obtained with 406.7-nm excitation using a Kr^+ laser (Coherent, Innova 90). The laser power was 10 mW. All spectra were recorded at 4 °C. The laser light was focused on the sample by a lens with a focal length of 50 mm. The resonance Raman scattering was detected with a spectrometer (Spex 1877 triplemate) in combination with a liquid nitrogen-cooled CCD detector (EG&G OMA 4, model 1530-CUV-1024S).

Stopped-Flow Analysis of the Reaction of ODQ with β1-(1−385). β1(1−385) (100 μL, 10 μM in 50 mM Hepes, pH 7.4, and 100 mM NaCl) was mixed with 100 μL of various concentrations of ODQ in a Hi-Tech stopped flow instrument at room temperature. The reaction was monitored by absorbance changes at 431 or 392 nm. The stopped-flow traces were fit to a single exponential, and apparent rate constants (k_{obs}) were obtained. The second-order rate constant for ODQ reacting with β1(1−385) was obtained by plotting the k_{obs} versus ODQ concentrations using the equation $k_{obs} = k_f$ [ODQ].

RESULTS

Electronic Absorption Spectra of ODQ-Treated sGC. sGC isolated from the baculovirus/Sf9 expression system contains a ferrous, 5-coordinate, high-spin heme with a Soret peak at 431 nm and a single α/β band at 562 nm (Figure 2A), which is identical to that of sGC purified from bovine lung (*17*). Upon mixing sGC with ODQ, the Soret peak shifted from 431 to 392 nm (Figure 2A). The α/β region also changed from a single peak at 562 nm to two peaks at 514 and 652 nm. Identical spectral changes were observed when sGC was treated with ferricyanide (data not shown) and are identical to those previously reported for the oxidized enzyme (*18*). These results suggest that the heme in sGC is oxidized by ODQ.

Effects of ODQ on sGC Basal Activity. As shown in Table 1, in the absence of NO, ferrous sGC had a specific activity of 68 ± 12 nmol min^{-1} mg^{-1} consistent with previously published data (*16*). When the sGC sample was treated with ODQ, sGC retained a specific activity that was within experimental error of the untreated enzyme (88 ± 11 nmol min^{-1} mg^{-1}) (Table 1), suggesting that even though ODQ oxidized the heme, it had very little effect on the basal catalytic activity.

Data shown in Table 1 were obtained in the absence of ODQ in the activity assay mixture (sGC was treated with ODQ, and ODQ was then removed by gel filtration). In another set of experiments, different concentrations of ODQ were added to sGC assay mixtures. ODQ did not significantly alter sGC basal activity up to an ODQ concentration of 100 μM (data not shown). In the presence of NO, ferrous sGC was activated 331-fold to a specific activity of 22541 ± 2095 nmol min^{-1} mg^{-1}. The ODQ-treated sGC had a much lower NO-stimulated activity of 43-fold over basal.

Reversibility of the ODQ Effect. ODQ-oxidized sGC could be re-reduced by dithionite. The electronic absorption spectrum of this re-reduced sGC was identical to that of ferrous sGC as isolated (Figure 2, panels B and C). This re-reduced sGC had slightly higher basal activity (about 2-fold) as compared to untreated enzyme but had the same NO-stimulated activity within experimental error (Table 1).

Spectral Characterization of Reactions of NO with ODQ-Treated sGC. ODQ-treated sGC has a Soret peak at 392 nm and α/β peak at 514 and 652 nm (Figure 2). Anaerobic addition of NO gas to ODQ-treated sGC at 10 °C did not result in any optical spectral changes (data not shown). However, under turnover conditions at 37 °C, NO induced electronic absorption spectral changes. The Soret peak was slightly red-shifted and decreased in extinction, with additional changes in the α/β region (data not shown). The

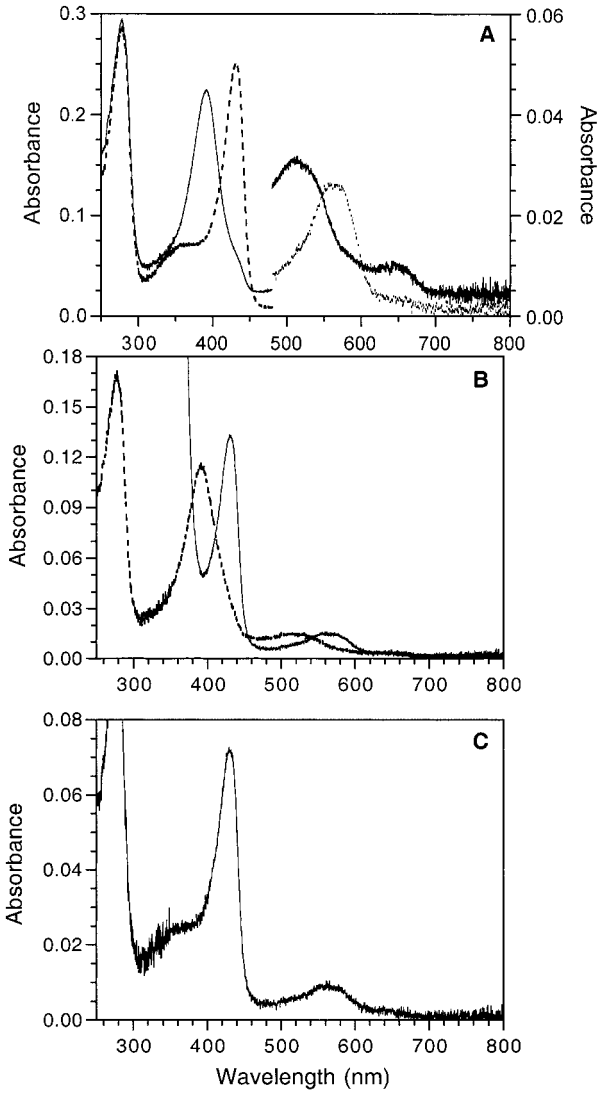

FIGURE 2: Electronic absorption spectrum of ODQ-treated sGC. (A) sGC (1.8 μM) in 50 mM Hepes, pH 7.4, 50 mM NaCl: (····) ferrous sGC, and (−) ODQ-treated sGC. The left scale refers to the Soret and protein peak region, and the right scale refers to the α/β region. (B) 0.5 mL of 1.6 μM sGC was desalted into 20 HEPES, pH 7.4, and 50 mM NaCl, concentrated to 0.5 mL (1.45 μM) and oxidized with 1 μL of 870 μM ODQ in DMSO for 10 min at 10 °C and then ~10 grains of sodium dithionite to give spectrum as shown. (C) Sample in panel B was desalted on a PD-10 column (Bio-Rad) and then concentrated (Ultrafree-15 50K Millipore spin concentrator) to 0.4 mL giving the spectrum as shown.

spectral changes could be due to formation of a ferric−nitrosyl complex or formation of a ferrous−nitrosyl complex or both. Examination of this sample by EPR spectroscopy clearly showed the presence of ferrous−nitrosyl sGC (Figure 3). The spectrum shown in Figure 3 is identical to the previously published EPR spectra of 5-coordinate ferrous−nitrosyl sGC complex (*9*).

Effects of ODQ on Electronic Absorption Spectrum of β1-(1−385). Addition of ODQ to β1(1−385) also led to a shift in the Soret peak to 392 nm and split the α/β band as for sGC (data not shown). Anaerobic addition of ODQ also led to the same spectral change (data not shown).

EPR Characterization of ODQ Oxidized β1(1−385). The EPR spectrum of ODQ-treated β1(1−385) is shown in Figure 4. The EPR data indicate that the heme in the ODQ-treated β1(1−385) is ferric and high-spin. Computer simulation of the EPR spectrum generated *g* values of 6.75, 5.48, and 1.99 with line widths of 44, 50, and 27 G, respectively. These *g* values are similar to those reported for ferric sGC generated by oxidation of bovine lung sGC with ferricyanide (*18*).

Table 1: Specific Activities of Ferric and Ferrous sGC

sGC sample	basal activity (nmol min^{-1} mg^{-1})	NO-stimulated activity (nmol min^{-1} mg^{-1})	fold activation
ferrous sGC as isolated	68 ± 12	22 541 ± 2095	331
ODQ-oxidized sGC[a]	88 ± 11	3804 ± 593	43
re-reduced sGC[b]	157 ± 14	20 091 ± 441	128

[a] sGC was preincubated with ODQ, desalted in 50 mM Hepes, pH 7.4, and 50 mM NaCl, and then assayed in the absence of ODQ. [b] sGC was incubated with ODQ and desalted to remove ODQ, sodium dithionite was used to rereduce sGC heme, and rereduced sGC was desalted again and then assayed in the absence of both dithionite and ODQ.

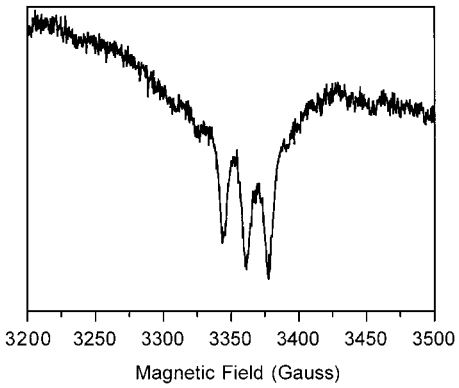

FIGURE 3: EPR characterization of reactions of ODQ-treated sGC with NO. EPR spectrum of ODQ-treated sGC in the presence of 1 mM DEA-NONOate, 50 mM Hepes, pH 7.4, 5 mM $MgCl_2$, and 1.5 mM GTP, and 10% glycerol. EPR conditions were as follows: temperature, 25 K; microwave frequency, 9.5 GHz; microwave power, 2 mW; modulation amplitude, 4 G. The slight baseline deviation observed is the result of a trace contamination of copper in the cavity.

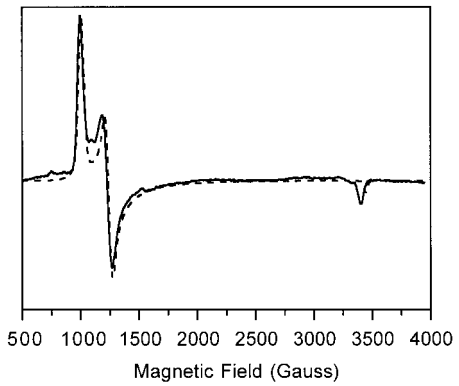

FIGURE 4: EPR spectrum of the ODQ-oxidized β1(1−385) (160 μM in 50 mM Hepes, pH 7.4, 100 mM NaCl, and 10% glycerol). EPR experimental conditions were as follows: temperature, 10 K; microwave frequency, 9.477 GHz; microwave power, 20 mW; modulation amplitude, 32 G. EPR spectra were simulated using the program Simfonia (version 1.0) from Bruker, and *g* values of the heme signal are 6.75, 5.48, and 1.99, with line widths of 44, 50, and 27 G, respectively.

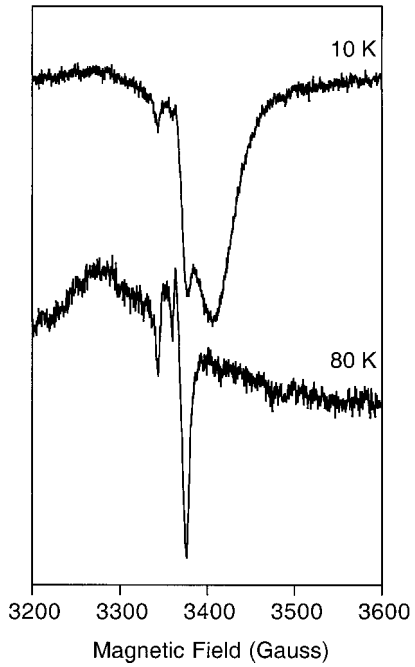

FIGURE 5: Temperature dependence of the EPR spectrum of the ODQ-treated β1(1−385). The top spectrum was taken at 10 K, while the bottom spectrum was recorded at 80 K for the same sample. The final concentration of β1(1−385) and ODQ was 160 and 320 μM, respectively.

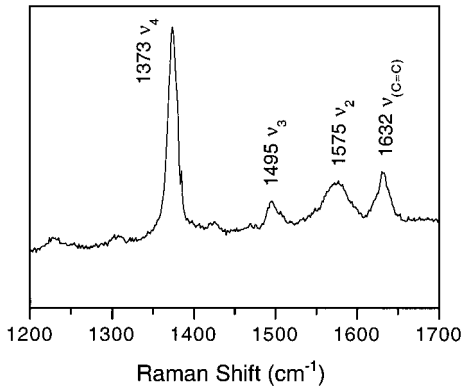

FIGURE 6: Resonance Raman spectrum of the ODQ-treated β1-(1−385). Final concentrations were β1(1−385), 25 μM and ODQ, 30 μM, and the accumulation time was 5 min.

Further EPR Characterization. Since the ferrous heme of sGC is one electron oxidized by ODQ, we investigated whether an organic radical could be detected. We recorded the EPR spectrum of ODQ-treated β1(1−385) at both 10 and 80 K (Figure 5). At 80 K, the ferric heme signal is not visible while that from an organic radical can still be observed. At 10 K, the spectrum at $g = 2.0$ appears to be a mixture of signals from both ferric heme and an organic radical. At 80 K, the heme signal disappeared, leaving a species consistent with an organic radical as the predominant signal with a width of 59 G and a g value near 2 (Figure 5).

Resonance Raman Spectrum of ODQ-Treated β1(1−385). The resonance Raman spectrum of ODQ-treated β1(1−385) is shown in Figure 6. It has an intense peak at 1373 cm^{-1} (ν_4) that is sensitive to the oxidation state of the heme. Ferric heme usually has a ν_4 around 1372 cm^{-1}, while ferrous heme has a ν_4 around 1356 cm^{-1}. ODQ-treated β1(1−385) also has a ν_3 at 1495 cm^{-1}, ν_2 at 1575 cm^{-1}, and a $\nu_{(C=C)}$ at 1632 cm^{-1}. The Raman spectrum indicates that the ODQ-treated

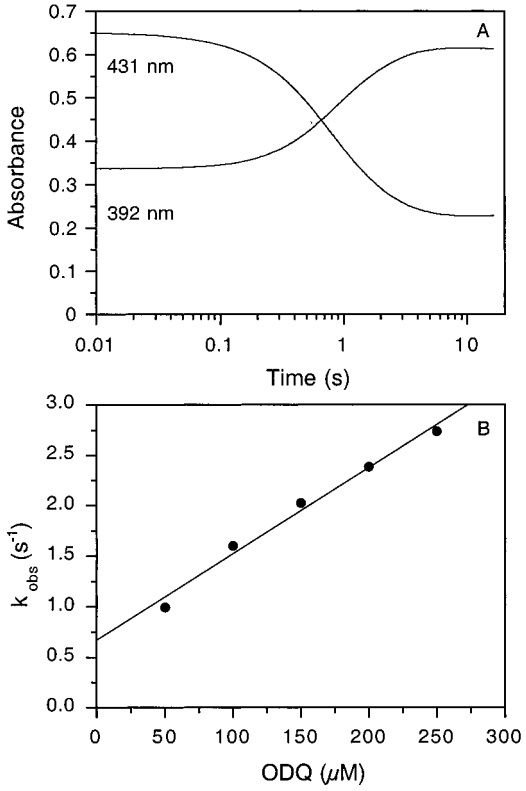

FIGURE 7: Stopped-flow analysis of the reaction of ODQ with β1-(1−385). (A) Stopped-flow traces obtained at 431 and 392 nm. Protein and ODQ concentrations were 10 and 100 μM, respectively. (B) Plot of the observed rate constants (k_{obs}) versus ODQ concentration.

β1(1−385) heme is ferric, 5-coordinate, and high-spin, which is consistent with our EPR and electronic absorption spectroscopy observations (*19*). Some evidence of low-spin heme can be seen in Figure 6. In fact, ferric β1(1−385) is relatively unstable and slowly converts to a low-spin form in the spectrometer.

Oxidation Rate of β1(1−385) by ODQ. The kinetics of β1(1−385) oxidation by ODQ was followed by the shift of the Soret peak from 431 to 392 nm. Two typical stopped-flow traces obtained at 431 and 392 nm are shown in Figure 7A. ODQ caused a decrease in absorbance at 431 nm and an increase in absorbance at 392 nm. The stopped-flow traces were fit to single exponentials, and pseudo-first-order rate constants (k_{obs}) were obtained. A replot of k_{obs} versus the ODQ concentration (Figure 7B) gave a value for the bimolecular reaction rate constant of 8.5×10^3 M^{-1} s^{-1}. The data shown in Figure 7A also indicate that no detectable intermediate was formed during the course of β1(1−385) oxidation.

DISCUSSION

ODQ is widely used as a specific inhibitor of sGC in pharmacological studies of the NO/cGMP pathway (*11*, *13*, *20*−*25*). The goal of this study was to understand the molecular mechanism of the inhibitory effects of ODQ on sGC and to determine the nature of the reported specificity of inhibition. It had previously been shown that binding of ODQ to sGC shifted the Soret peak from 431 to 392 nm, suggesting that the heme in sGC had been oxidized (*11*). Here we provide conclusive evidence that the hemes in both

ODQ-treated sGC and β1(1−385) are ferric. Addition of ODQ to β1(1−385) led to the appearance of a typical ferric heme EPR spectrum (Figure 4), which is identical to that previously reported for ferric heterodimeric sGC (*18*). In addition, the resonance Raman spectrum of the ODQ-treated β1(1−385) had a ν_4 at 1373 cm^{-1} and a ν_3 at 1495 cm^{-1} (Figure 6), which indicated that the heme was ferric.

There are two plausible mechanisms that could explain the oxidation of sGC heme by ODQ. First, ODQ could bind to sGC and cause a conformational change that increases the affinity of sGC for oxygen. The resulting ferrous oxygen complex might undergo autoxidation to generate ferric heme and superoxide. In fact, we have evidence obtained through the use of a β1(1−385) point mutant, H105G, showing that autoxidation of the ferrous heme is fast when oxygen binds (*7*). However, it is unlikely that this mechanism is responsible for heme oxidation because anaerobic addition of ODQ to β1(1−385) also led to oxidation of the heme (data not shown). In addition, the fact that no ferrous−oxy intermediate was observed when ODQ was mixed with β1(1−385) in a stopped-flow instrument (Figure 7A) suggests that this mechanism is unlikely. A second mechanism involves direct transfer of an electron from sGC to ODQ to generate an ODQ radical. When β1(1−385) was mixed with ODQ in an EPR tube and immediately frozen in liquid nitrogen, a radical signal was observed (Figure 5). This signal is consistent with the species being an organic radical. When the temperature is increased from 10 to 80 K to decrease the heme signal, the signal becomes much sharper, also suggestive of an organic radical. This organic radical is likely an ODQ radical or protein-based radical, perhaps derived from an initial ODQ radical. Definitive assignment of this radical requires further studies.

The apparent oxidant action of ODQ led us to consider other reactions that were likely in vivo. Although the chemistry of the reaction is clearly different (reaction with an oxyheme complex), we decided to test if it would oxidize oxyhemoglobin. When ODQ was mixed with ferrous oxyhemoglobin, the Soret shifted from 415 to 406 nm (data not shown), suggesting oxidation of the hemoglobin heme. Although the mechanism of hemoglobin oxidation by ODQ has not been determined here, it is clear that this reaction will complicate interpretation of pharmacological data when ODQ is used in vivo or with crude samples. This is consistent with tissue and cell extract studies that indicated that ODQ interferes with other heme-dependent processes (*26*). Also, recent work by Wegener and co-workers found that excess myoglobin abolished the inhibitory effect of ODQ on sGC in cytosolic extracts from cardiomyocytes (*21*). The authors suggested that myoglobin could bind ODQ, so preventing its action on sGC and accounting for the failure of ODQ to inhibit sGC in rat ventricular cardiomyocytes. In light of the data presented here, the most likely explanation for these observations is that oxymyoglobin, like oxyhemoglobin, is able to react with, and effectively inactivate, ODQ. Although with ODQ there is an apparent lack of specificity for sGC versus other hemoproteins, this small molecule can be used as a starting point in the design of a more specific compound.

ODQ has been reported to inhibit sGC basal activity (*14*). It is not clear whether inhibition arose as a result of disruption of the catalytic site or conversion of sGC to an oxidized form with a lower specific activity. Here we showed that sGC is oxidized by ODQ under basal assay conditions and that the resulting ferric sGC had slightly increased specific activity. This is consistent with previous studies from our laboratory on ferric sGC (*18*).

As in previous studies, ODQ-treated sGC had much lower NO-stimulated activity. The specific activity of ODQ-oxidized sGC in the presence of NO was 3804 ± 593 nmol min^{-1} mg^{-1}, as compared to 22 541 ± 2095 nmol min^{-1} mg^{-1} for ferrous sGC plus NO. Inhibition of the NO-stimulated activity by ODQ is not due to the inactivation of the catalytic site since ODQ-oxidized sGC can be re-reduced by dithionite and subsequently activated by NO to the same level as the original ferrous sGC (Table 1). Since ODQ does not perturb the catalytic site, the inhibitory effects of ODQ on the NO-stimulated sGC activity likely results from oxidation of the heme in sGC or reaction of ODQ with NO. The possibility that inhibition of the NO-stimulated sGC activity results from reaction of ODQ with NO can be ruled out: When sGC is incubated with ODQ and then desalted, the resulting ferric sGC has much lower NO-stimulated activity, although there is no ODQ present in the assay. Therefore, inhibition of NO-stimulated sGC activity is almost certainly due to oxidation of the sGC heme. Using an NO electrode, others also came to the conclusion that ODQ and NO do not directly react (*11*). NO binds to ferric heme much more slowly than to ferrous heme, but that arises because the slow step in the reaction is H_2O or ^-OH dissociation that must occur prior to NO binding (*27*). Since the ferric forms of sGC and β1(1−385) are high-spin and 5-coordinate, the on-rate of NO is likely to be about the same as the respective ferrous forms. The overall affinity of NO for ferric hemoproteins, however, is much lower than for ferrous hemoproteins. For example, the K_d for NO binding to ferrous myoglobin at 20 °C is 7.0×10^{-12} M, while for ferric myoglobin the K_d is 2.6×10^{-4} M (*28*, *29*). Thus, oxidation of sGC heme will lead to a lower NO affinity. It is unknown how the specific activity of the ferric−nitrosyl sGC complex would compare to that of the ferrous−nitrosyl sGC complex.

ODQ-treated sGC retained significant NO-stimulated activity (Table 1). There are two possible explanations for this observation. First, it is possible that the ferric−nitrosyl complex has some NO stimulated-activity, but it is much lower than that of ferrous−nitrosyl sGC complex. An alternative explanation is that the ferric−nitrosyl sGC complex is not stable and converted to ferrous−nitrosyl complex in the presence of excess NO. There is precedent for this process in the hemoglobin literature. Hoshino and co-workers found that autoreduction of ferric−nitrosyl hemoglobin was first-order with respect to hydroxide with a bimolecular rate constant of 3.2×10^3 M^{-1} s^{-1} (*30*). The latter explanation is more likely since we observed formation of a ferrous−nitrosyl complex in the presence of NO under turnover conditions (Figure 3). This fraction of ferrous−sGC could explain the observed partial activation of the ODQ-treated sGC by NO. A working hypothesis is shown in Figure 8 that takes into account the observations here as well as previously published work.

In summary, we have conclusively shown that ODQ can oxidize the heme moiety in sGC without adversely affecting the catalytic domain. The inhibitory effect of ODQ on NO-stimulated sGC activity is most likely due to the change of the oxidation state of the sGC heme. Since sGC is the only

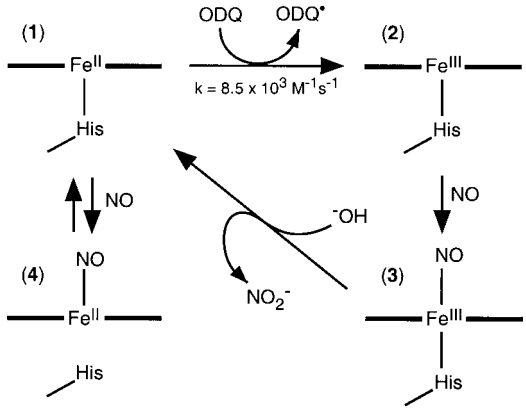

FIGURE 8: Model for redox regulation of sGC by ODQ and NO. Unactivated ferrous sGC (**1**) can bind NO to form the activated ferrous−nitrosyl form of sGC (**4**). Reaction of **1** with ODQ results in oxidized sGC heme (**2**) and generation of an ODQ radical species. We suggest that NO can bind to ferric sGC to form a ferric−nitrosyl species (**3**), which undergoes a rapid reaction to yield ferrous sGC (**1**) with net loss of NO^+. Literature precedent (see main text) indicates that this process involves reaction with hydroxide to generate nitrite. The re-reduced sGC can once again be activated by NO.

heme-containing cyclase among all the nucleotide cyclases, the heme site specific inhibitor, ODQ, is a useful tool to distinguish signal transduction events mediated by sGC from those involving other nucleotide cyclases. However, the nonspecific reaction of ODQ with other hemoproteins will complicate the use of ODQ in vivo. The mechanism of ODQ inhibition suggests a generalized approach toward sGC inhibition that would be based on selective interaction and oxidation of the heme moiety.

ACKNOWLEDGMENT

We thank Bryan Schmidt for assistance with EPR characterization of the reaction of ODQ-treated sGC with NO. We also thank members of the Marletta lab for critical evaluation of this manuscript.

REFERENCES

1. Garbers, D. L., and Lowe, D. G. (1994) *J. Biol. Chem. 269*, 30741−30744.
2. Denninger, J. W., and Marletta, M. A. (1999) *Biochim. Biophys. Acta 1411*, 334−350.
3. Garbers, D. L. (1979) *J. Biol. Chem. 254*, 240−243.
4. Gerzer, R., Böhme, E., Hofmann, F., and Schultz, G. (1981) *FEBS Lett. 132*, 71−74.
5. Wedel, B., Humbert, P., Harteneck, C., Foerster, J., Malkewitz, J., Bohme, E., Schultz, G., and Koesling, D. (1994) *Proc. Natl. Acad. Sci. U.S.A. 91*, 2592−2596.
6. Zhao, Y., and Marletta, M. A. (1997) *Biochemistry 36*, 15959−15964.
7. Zhao, Y., Schevis, J., Babcock, G. T., and Marletta, M. A. (1998) *Biochemistry 37*, 4502−4509.
8. Wedel, B., Harteneck, C., Foerster, J., Friebe, A., Schultz, G., and Koesling, D. (1995) *J. Biol. Chem. 270*, 24871−24875.
9. Stone, J. R., Sands, R. H., Dunham, W. R., and Marletta, M. A. (1995) *Biochem. Biophys. Res. Commun. 207*, 572−577.
10. Ignarro, L. J., Degnan, J. N., Baricos, W. H., Kadowitz, P. J., and Wolin, M. S. (1982) *Biochim. Biophys. Acta 718*, 49−59.
11. Garthwaite, J., Southam, E., Boulton, C. L., Nielsen, E. B., Schmidt, K., and Mayer, B. (1995) *Mol. Pharmacol. 48*, 184−188.
12. Olesen, S., Drejer, J., Axelsson, O., Moldt, P., Bang, L., Nielsen-Kudsk, J. E., Busse, R., and Mülsch, A. (1998) *Br. J. Pharmacol. 123*, 299−309.
13. Guerra de Gonzalez, L., Misle, A., Pacheco, G., Napoleon de Herrera, V., Gonzalez de Alfonzo, R., Lippo de Becemberg, I., and Alfonzo, M. J. (1999) *Biochem. Pharmacol. 58*, 563−569.
14. Schrammel, A., Behrends, S., Schmidt, K., Koesling, D., and Mayer, B. (1996) *Mol. Pharmacol. 50*, 1−5.
15. Buechler, W., Singh, S., Aktas, J., Muller, S., Murad, F., and Gerzer, R. (1995) *Adv. Pharmacol. 34*, 293−303.
16. Brandish, P. E., Buechler, W., and Marletta, M. A. (1998) *Biochemistry 37*, 16898−16907.
17. Stone, J. R., and Marletta, M. A. (1994) *Biochemistry 33*, 5636−5640.
18. Stone, J. R., Sands, R. H., Dunham, R., and Marletta, M. A. (1996) *Biochemistry 35*, 3258−3262.
19. Schelvis, J. P. M., Zhao, Y., Marletta, M. A., and Babcock, G. T. (1998) *Biochemistry 37*, 16289−16297.
20. Brunner, F., Stessel, H., and Kukovetz, W. R. (1995) *FEBS Lett. 376*, 262−266.
21. Wegener, J. W., Closs, E. I., Forstermann, U., and Nawrath, H. (1999) *Br. J. Pharmacol. 127*, 693−700.
22. Homer, K. L., Fiore, S. A., and Wanstall, J. C. (1999) *J. Pharm. Pharmacol. 51*, 135−139.
23. Hwang, T. L., Wu, C. C., and Teng, C. M. (1998) *Br. J. Pharmacol. 125*, 1158−1163.
24. Onoue, H., and Katusic, Z. S. (1998) *Brain Res. 785*, 107−113.
25. Hussain, A. S., Marks, G. S., Brien, J. F., and Nakatsu, K. (1997) *Can. J. Physiol. Pharmacol. 75*, 1034−1037.
26. Feelisch, M., Kotsonis, P., Siebe, J., Clement, B., and Schmidt, H. H. (1999) *Mol. Pharmacol. 56*, 243−253.
27. Sharma, V. J., Traylor, T. G., and Gardiner, R. (1987) *Biochemistry 26*, 3837−3843.
28. Moore, E. G., and Gibson, Q. H. (1976) *J. Biol. Chem. 251*, 2788−2794.
29. Cooper, C. E. (1999) *Biochim. Biophys. Acta 1411*, 290−309.
30. Hoshino, M., Maeda, M., Konishi, R., Seki, H., and Ford, P. C. (1996) *J. Am. Chem. Soc. 118*, 5702−5707.

BI9929296